Journal of the Neurological Sciences 400 (2019) 129–134

Contents lists available at ScienceDirect

Journal of the Neurological Sciences

journal homepage: www.elsevier.com/locate/jns

Differences in the intra-cerebellar connections and graph theoretical measures between Parkinson's disease and multiple system atrophy

Wataru Sako[a,*], Takashi Abe[b], Takahiro Furukawa[a], Ryosuke Oki[a], Shotaro Haji[a], Nagahisa Murakami[a], Yuishin Izumi[a], Masafumi Harada[b], Ryuji Kaji[a]

[a] Department of Clinical Neuroscience, Institute of Biomedical Sciences, Tokushima University Graduate School, Tokushima, Japan
[b] Department of Radiology, Institute of Biomedical Sciences, Tokushima University Graduate School, Tokushima, Japan

ARTICLE INFO

Keywords:
Parkinson's disease
Multiple system atrophy
Functional magnetic resonance imaging
Graph theory
Cerebellum

ABSTRACT

Background and purpose: Parkinson's disease (PD) does not present with motor symptoms until dopaminergic neuronal loss exceeds 50%. This might indicate that a network-level compensatory mechanism involving surviving regions in PD acts to reduce brain abnormalities. In contrast, there is no evidence of a compensatory mechanism in multiple system atrophy (MSA). We hypothesized that a comparison of these two diseases would help to identify compensatory effects in PD.

Methods: We recruited 23 patients with PD, 11 patients with MSA, and 11 controls that showed an aging brain but no neurological deficits. All subjects underwent resting state functional magnetic resonance imaging (fMRI). Regions of interest were defined according to the motor network related to the basal ganglia and cerebellum. Network-level analyses were performed.

Results: Network-based statistical analyses revealed that functional connectivity in PD brains was reduced between cerebellar lobules IX on both sides and vermis X, as compared with MSA brains. Transitivity was reduced in MSA as compared with controls.

Conclusion: We demonstrated that a part of the intra-cerebellar connectivity was reduced in PD, and that network segregation was reduced in MSA. However, there was no evidence of compensatory effects in PD.

1. Introduction

Parkinson's disease (PD) is recognized as a combined disease that displays both motor and non-motor symptoms. PD presents with akinesia/bradykinesia, rigidity, resting tremor and postural instability as motor symptoms [1]. The motor symptoms are thought to be caused mainly by dopaminergic cell loss in the substantia nigra pars compacta, as levodopa, a precursor of dopamine, alleviates motor symptoms in patients with PD. Dopamine is important in controlling neuronal activity in the basal ganglia. Nonetheless, motor symptoms are not manifested in PD until dopaminergic cell loss exceeds 50% [2]. Therefore, compensatory mechanisms must play a role in the presymptomatic phase in order for such marked depletion to take place without symptomatic manifestations [3]. It is possible that network-level modification could contribute to such a compensatory mechanism. In multiple system atrophy (MSA), degeneration affects a wide range of neurons, such as the striatum, substantia nigra, pontine nuclei, inferior olive, and cerebellum [4,5], which suggests that no regions are left to provide a compensatory mechanism. Therefore, there is no evidence of the network-level compensatory mechanism in MSA, and comparison between PD and MSA could uncover network-level compensatory mechanism in PD.

Functional activity/connectivity in the basal ganglia circuits is altered by a lack of dopamine in PD, which is thought to induce motor symptoms [6]. Accumulating evidence has suggested the involvement of the cerebellum in motor symptoms in terms of compensatory effects [3,7], and the cerebellum is one of the main lesions in patients with MSA [4,5]. [18F]fluoro-2-deoxy-d-glucose positron emission tomography (FDG PET) and functional magnetic resonance imaging (fMRI) can detect functional abnormalities in PD [8,9]. In these imaging modalities, the whole brain is considered as a mass consisting of associated voxels, and several networks can be identified according to algorithms that are based on principal component analysis, independent component analysis, or graph theory [10–13]. These novel methods have demonstrated several network-level abnormalities in PD brains, which included elevated activities of the cerebellum [14–16]; this was in contrast to reduced activity of the cerebellum in MSA due to cerebellar degeneration [16]. Additionally, functional analytical

* Corresponding author at: 2-50-1 Kuramoto-cho, Tokushima 770-8503, Japan.
E-mail address: dwsako@tokushima-u.ac.jp (W. Sako).

https://doi.org/10.1016/j.jns.2019.03.022
Received 10 December 2018; Received in revised form 13 March 2019; Accepted 24 March 2019
Available online 25 March 2019

approaches have identified compensatory changes and network-level compensatory effects in other neurodegenerative diseases, such as amyotrophic lateral sclerosis and Huntington disease [17–19]. Given these findings, we hypothesized that abnormal activity in the basal ganglia circuits, due to a lack of dopamine, would be modulated by the cerebellum in a compensatory manner that differs between PD and MSA, and that this could be identified by resting state fMRI (RSfMRI). To test this hypothesis, we applied graph theoretical analyses of RSfMRI data from patients with PD or MSA to motor networks related to the basal ganglia and cerebellum.

2. Materials and methods

2.1. Subjects

A total of 45 subjects were recruited from the Department of Neurology of the Tokushima University Hospital. Twenty-three patients with PD met the UK Brain Bank criteria (12 men and 11 women, age: 67 ± 1.7 [mean ± standard error]), while 11 patients were diagnosed with MSA according to the consensus criteria (6 men and 5 women, age: 59 ± 2.2) [20]. Furthermore, 11 subjects who showed an aging brain on structural MRI, but no neurological deficits, were defined as controls (6 men and 5 women, age: 67 ± 3.2). The clinical characteristics of the included subjects are shown in Table 1. Informed consent was obtained from all participants under protocols approved by the local ethics committee.

All subjects underwent MRI scans of the brain. MRI was performed during the off-state in patients with PD, to minimize the effect of drugs. Disease duration was defined from the onset of motor symptoms to the time of the MRI scan for both patients with PD and those with MSA [21]. The disease severity of parkinsonian symptoms was evaluated using the Hoehn and Yahr scale (HY). All drugs for PD were pooled in levodopa equivalent doses (LED) according to the following modified version of a previously published formula: [22] levodopa/carbidopa × 1 + entacapone × 0.35 + pramipexole × 100 + ropinirole × 20 + rotigotine × 10 + selegiline × 10 + amantadine × 1. Other drugs were ignored due to limited efficacy.

2.2. MRI acquisition

MRI acquisition was performed essentially as previously reported [21]. Image acquisition was accomplished using a 3.0 T Discovery 750 scanner (GE, Milwaukee, WI). Scan parameters for RSfMRI were as follows: field of view (FOV) = 240 mm, matrix = 64 × 64, TR = 2000 ms, TE = 27.2 ms, flip angle = 77°, and slice thickness = 3.0 mm. Those of T1-weighted images were as follows: FOV = 240 mm, matrix = 256 × 256, TR = 7.77 ms, TE = 2.98 ms, flip angle = 8°, and slice thickness = 0.9 mm. All subjects were instructed to stay awake without making any movement, but to close their eyes while in the scanner.

2.3. Functional MRI analysis

For imaging analysis, the first four volumes were removed. All volumes then underwent motion correction, slice-timing correction, non-linear registration to the Montreal Neurological Institute (MNI-152: 2 × 2 × 2 mm^3) template following linear and non-linear registration of the structural image using FEAT in FMRIB's Software Library (FSL, http://www.fmrib.ox.ac.uk/fsl/). The subjects who showed head motion > 3 mm were excluded. Spatially normalized images were then smoothed using an 8 × 8 × 8 mm^3 kernel, using Statistical Parametric Mapping 8 (SPM8) software (http://www.fil.ion.ucl.ac.uk/spm/). CONN toolbox (http://www.nitrc.org/projects/conn) was used for band-pass filtering, denoising, and creating an adjacency matrix. As described elsewhere [21], the time series for each voxel was temporally band-pass filtered (0.01–0.08 Hz) to remove the effects of very-low-frequency drift and high frequency respiratory and cardiac noise. Moreover, a linear regression model was applied to remove unwanted motion and other artifactual effects, and for adjusting confounders including the BOLD signal from the white matter and cerebrospinal fluid and head motion. After adjustment, the histogram plots indicating the voxel-to-voxel connectivity were visually assessed to ensure that they were centered for each subject.

First, 132 automatic-anatomical-labeling (AAL) regions of interest (ROI) were used for whole brain analysis [23]. Of 132 AAL ROIs, 38 were selected on the basis of motor networks related to the basal ganglia and cerebellum (Supporting Table S1). Previous studies have utilized whole ROIs covering the brain or cerebral cortices only for graph theoretical analysis [24–29]. In the present study, we chose 38 ROIs according to our hypothesis that there would be a difference between PD and MSA in terms of motor-related connectivity, including the basal ganglia and cerebellum. The major advantage of using selected ROIs was dimension reduction, which could decrease the probability of type I error due to multiple testing. The second advantage was to maximize differences between groups in network-level values derived from graph theory, if our hypothesis proved correct. ROI-to-ROI functional connectivity values were calculated as adjacency matrix using Fisher-transformed correlation coefficients. The network-based statistic (NBS) was used to assess group differences in whole brain and motor networks related to the basal ganglia and cerebellum [13]. The NBS allowed for cluster-based statistical analysis in topological space, which consisted of nodes (ROIs) and edges between nodes, and provided family-wise error rate (FWER)-adjusted P value for each component using permutation testing (10,000 permutations). Component size was measured as the sum of test statistic values across all connections comprising the component. The test statistic threshold was set at 3.5.

Network-level properties were assessed by transitivity, characteristic path length, degree, and assortativity after binarization of the adjacency matrices. Transitivity is the normalized clustering coefficient based on the number of triangles in the networks, which allows for measurement of functional segregation [30]. The characteristic path length of the network is the average shortest path length between all pairs of nodes in the network, and is the most commonly used measure of functional integration [30]. The degree is the number of links connected to a node, and is a measure of centrality [30]. The assortativity coefficient is a correlation coefficient between the degrees of all nodes on two opposite ends of a link, and is considered as a measure of resilience [30]. The above-mentioned process was performed using a package of igraph (https://cran.r-project.org/web/packages/igraph/

Table 1
Characteristics of the subjects recruited in this study.

Group	Age-yr	Male (Female)	Handedness Right (Left)	Disease Duration - years	HY	Tremor	Onset symptom Tremor (Others)	LED	MSA-P (MSA-C)
Ctr	67 ± 3.2	6 (5)	9 (2)	NA	NA	NA	NA	NA	NA
PD	67 ± 1.7	12 (11)	22 (1)	4.7 ± 0.71	2.0 ± 0.20	16	13 (10)	255 ± 48.7	NA
MSA	59 ± 2.2	6 (5)	10 (1)	2.8 ± 0.39	3.4 ± 0.48	0	0 (11)	NA	7 (4)

Abbreviations: Ctr, control; HY, Hoehn-Yahr stage; LED, levodopa equivalent dose; MSA, multiple system atrophy; MSA-C, MSA with predominant cerebellar ataxia; MSA-P, MSA with predominant parkinsonian feature; NA, not available; PD, Parkinson's disease. Mean ± standard error.

igraph.pdf) in R software (https://www.r-project.org/).

2.4. Statistical analyses

Analysis of variance (ANOVA) was utilized to compare the continuous variables among the 3 groups. Post-hoc analyses were conducted using Tukey's honestly significant difference (HSD) test. Pearson's product-moment correlation coefficients were calculated between measurements derived from network-level analyses and age, disease duration, HY, and LED, to clarify the relationship between factors. All statistical analyses were performed using IBM SPSS Statistics version 21 (IBM Corp., Armonk, NY).

3. Results

3.1. Whole brain analysis

No significant changes were observed in network-level values, including the transitivity, characteristic path length, degree, or assortativity (ANOVA, $P > 0.50$; Fig S1A–D). Transitivity in PD group and characteristic path length in MSA was positively correlated with LED and HY, respectively (PD, transitivity and LED, $r = 0.43$, $P = 0.04$; MSA, characteristic path length and HY, $r = 0.82$, $P = 0.03$; Supporting Table S2). However, the number of subjects included in the latter correlation analysis was only 7, which limited reliability of this result. There was no significant correlation between other values (Supporting Table S2). In addition, there was no significant cluster consisting of nodes and edges based on the NBS (data not shown).

3.2. Analysis of motor networks related to basal ganglia and cerebellum

The same tendency was observed in the motor networks related to the basal ganglia and cerebellum as in the whole brain network. Transitivity was decreased in the MSA group as compared with the Ctr group (ANOVA, $P = 0.02$; Tukey HSD, $P = 0.02$; Fig. 1A), and differences in other network-level values did not reach significance (Fig. 1B–D). The NBS revealed a significant difference in cerebellar lobule-vermis connections, including cerebellar lobules IX, and vermises III and X, which are almost symmetric: there was lower functional connectivity in the PD than in the MSA groups (NBS, $P = 0.02$; Fig. 2). Post-hoc analysis of these connections suggested that functional connectivity was weak in patients with PD, as compared with those with MSA, between vermis X and lobule IX on the left (Cereb9L-Ver10; ANOVA, $P = 0.01$; Tukey HSD, $P < 0.01$; Fig. 3A) and right (Cereb9R-Ver10; ANOVA, $P = 0.01$; Tukey HSD, $P < 0.01$; Fig. 3B) sides. Of note, the Ctr group showed almost neutral functional connectivity on these symmetric connections, while negative and positive connectivity was observed in the PD and MSA groups, respectively (Fig. 3A and B).

There was no significant difference in functional connectivity between lobule IX and vermis III among the groups (Cereb9R-Ver3; ANOVA, $P = 0.13$; Fig. 3C). Functional connectivity between lobules IX on both sides and vermis X negatively correlated with disease duration in PD group ($r = -0.45$, $P = 0.03$; Fig. 4). There was no significant correlation between other network-level values and age, disease duration, HY, or LED (Supporting Table S3).

4. Discussion

Our network-based analysis revealed that lobule-vermis connectivity, a part of the intra-cerebellar network, was reduced in the PD as compared with the MSA group, and was associated with disease duration. It was possible that our finding could be associated with compensatory effects because the direction of change in lobule-vermis connectivity was different between PD and MSA. Massive degeneration may deprive a compensatory mechanism of MSA, while surviving regions in PD may provide a compensatory mechanism. The functional connectivity should positively correlate with disease duration if our findings were associated with a compensatory mechanism, according to a hypothetical model of compensatory effects [7]. However, there was negative correlation, which might indicate that a change in lobule-vermis connectivity was not attributed to a compensatory mechanism. Using a new framework for studying the underlying abnormality in the motor network related to the basal ganglia and the cerebellum allowed detection of compensatory changes in the cerebellum in patients with PD. Technically, dimension reduction and the contrast to patients with MSA led to novel findings in this study, whereas previous studies using the NBS did not identify lesions in the cerebellum [25,29].

The ROIs used in the present study were fit to the motor network related to the basal ganglia and cerebellum, but the cerebellum is also involved in other functions, including cognition and emotion. Cerebellar lobule IX was reported to be associated with the visual guidance of movement and the default mode network [31,32]. Negative functional connectivity between lobule IX and vermis X in the PD group could contribute to visual hallucinations, while MSA does not present such negative functional connectivity or visual hallucinations.

In the present study, several network-level values were assessed in the motor network related to the basal ganglia and cerebellum, and transitivity was found to be decreased in MSA group as compared with Ctr group. Reduced transitivity generally indicates reduced network segregation and loss of specialized processing in the specific brain region [30]. Insufficient segregation in patients with MSA appeared plausible, because more severe MSA involves the loss of more specific functions than PD. This result was in line with that of a previous study that used diffusion tensor imaging [33]. However, characteristic path length was not increased in the present study, which could be attributed to differences between diffusion tensor imaging and functional imaging and/or between MSA with predominant cerebellar ataxia only and MSA. For PD group, there were no significant differences in transitivity, characteristic path length, degree, or assortativity, which appeared consistent with a previous study that reported that there were no significant differences in these network-level values when compared with normal controls [28]. However, another study reported that PD patients exhibited lower global efficiency, higher clustering coefficients, and higher characteristic path lengths than healthy controls [29]. Diverse backgrounds as well as differences in methodology may have contributed to the different results among the studies.

There were two major limitations to the present study. Due to the modest number of subjects, the study may have had insufficient statistical power. Although we focused on the motor network related to the basal ganglia and cerebellum, the subthalamic nucleus and the pontine nucleus were not used as ROIs. These two nuclei play a key role in connecting the basal ganglia to the cerebellum.

In conclusion, we here proposed a new framework for studying the underlying abnormality in the motor network related to the basal ganglia and cerebellum, using ROIs in the NBS, similar to other voxelwise analyses. Patients with PD were found to show reduced functional connectivity between cerebellar lobule IX and vermis X compared with those with MSA. Furthermore, transitivity, one of the network-level measurements derived from graph theory, was reduced in MSA, as reported previously based on diffusion tensor imaging. These findings shed light on the network-level changes in PD and MSA.

Supplementary data to this article can be found online at https://doi.org/10.1016/j.jns.2019.03.022.

Disclosure of interest

The authors report no conflict of interest concerning the materials or methods used in this study or the findings specified in this paper.

Acknowledgements

We would like to thank all subjects that recruited in the present

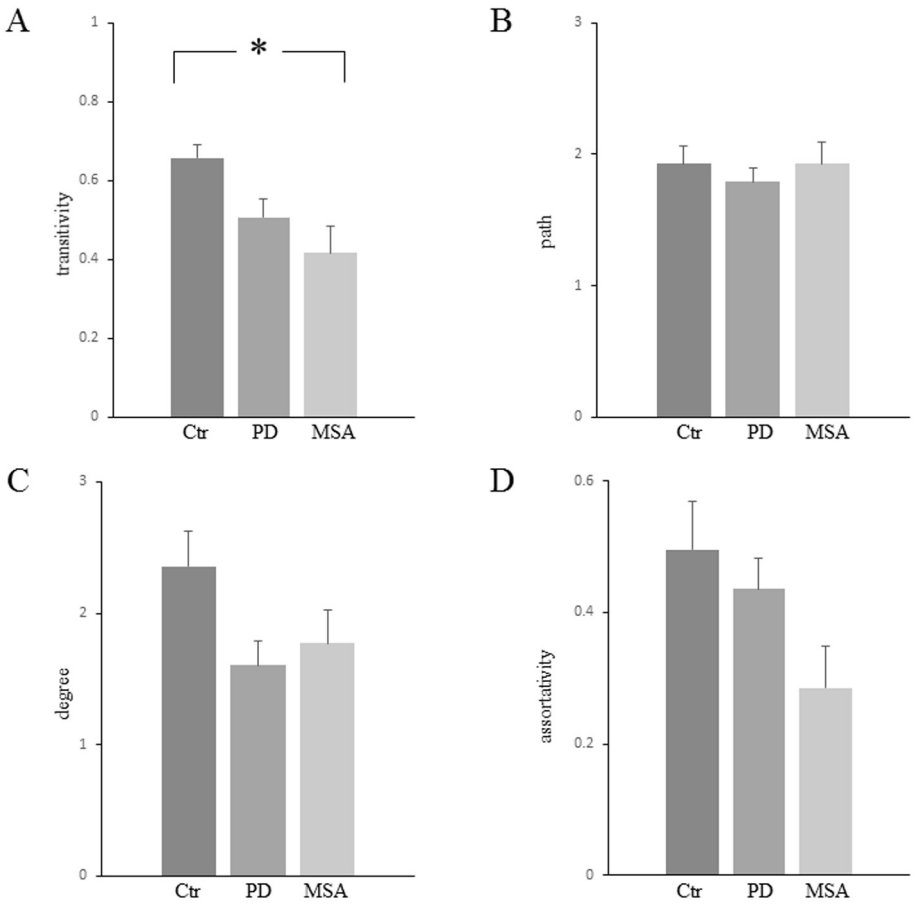

Fig. 1. Network-level analyses based on graph theory in the motor network related to basal ganglia and cerebellum. (A) MSA group showed significantly lower transitivity than the control (Ctr) group. (B-D) No significant difference in characteristic path length (B), degree (C) or assortativity (D) was seen among the groups, although the PD and MSA groups tended to exhibit reduced degree (C) and assortativity (D). *$P < 0.05$.

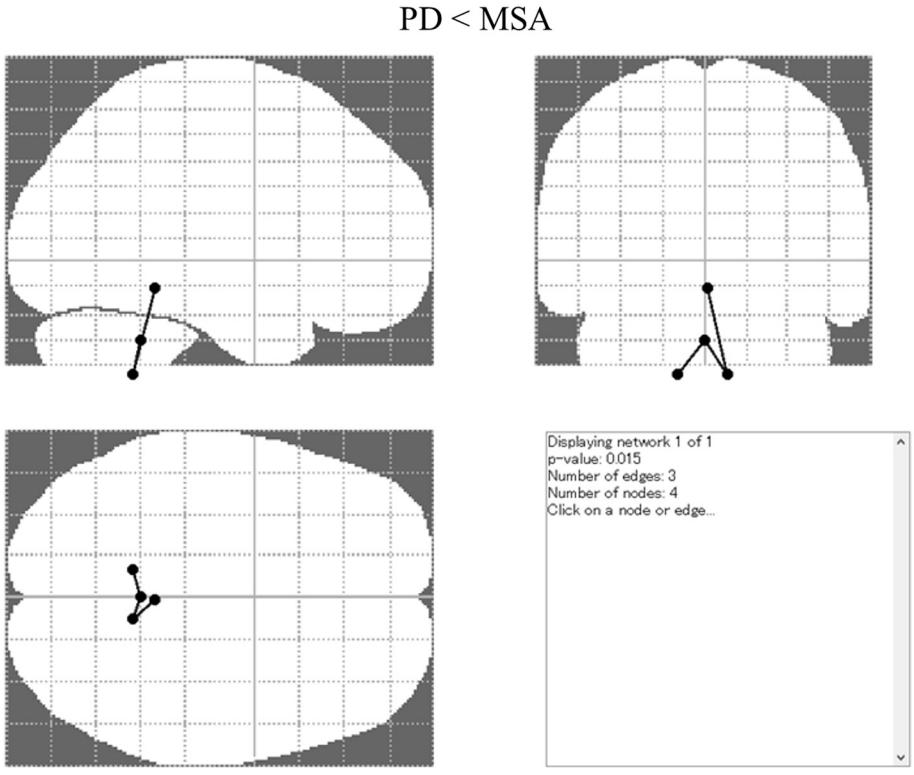

Fig. 2. Nodes and edges with reduced functional connectivity in patients with PD relative to those with MSA. Intriguingly, connections detected here demonstrated almost symmetry with the cerebellum. These nodes were the cerebellar lobules IX and vermises X and III.

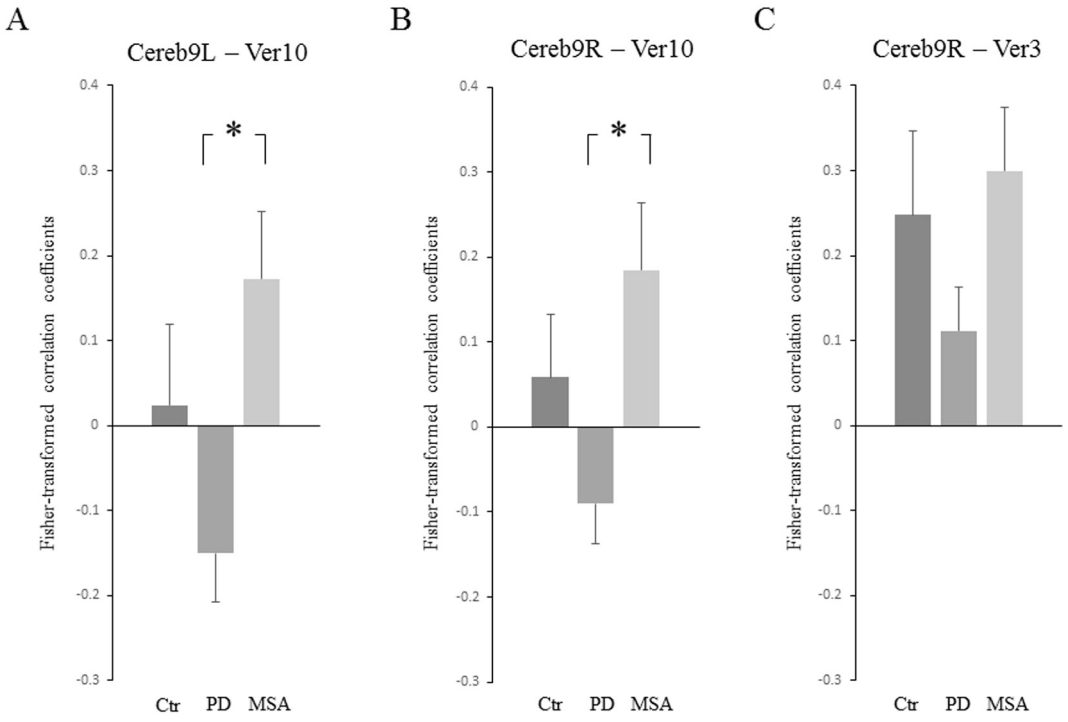

Fig. 3. Post-hoc analyses of selected connections by network-based statistics (NBS) in the cerebellum. (A) (B) There was significant difference in the functional connectivity of cerebellar lobules IX (Cereb9L and Cereb9R) with vermis X (Ver10) between the PD and MSA groups. (C) No significant difference was observed in functional connectivity between Cereb9R and vermis III (Ver3). *$P < 0.05$

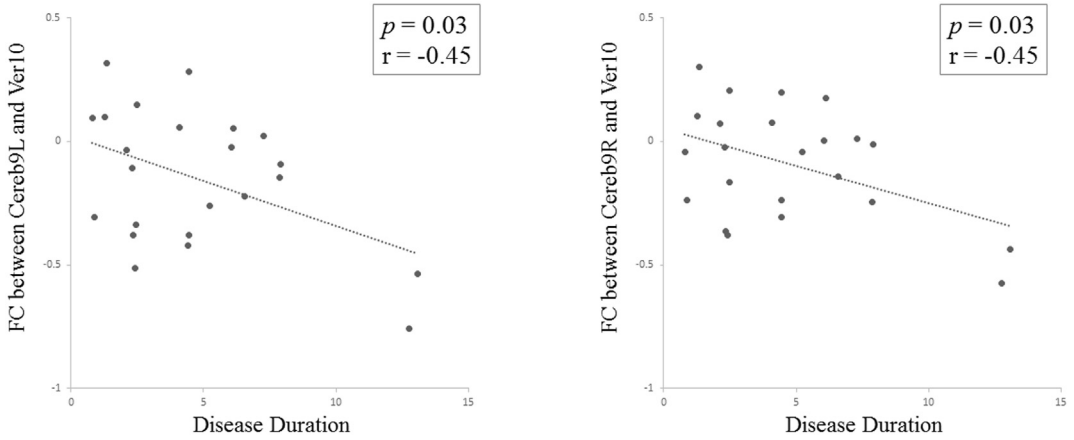

Fig. 4. Individual functional connectivity values (FC) between left/right cerebellar lobule IX (Cereb9L/R) and vermis X (Ver10) in PD group. FC between Cereb9L/R and Ver10 significantly correlated with disease duration.

study.

References

[1] L.V. Kalia, A.E. Lang, Parkinson's disease, Lancet (London, England). 386 (9996) (2015 Aug 29) 896–912 (PubMed PMID: 25904081. Epub 2015/04/24. eng.).

[2] J.H. Kordower, C.W. Olanow, H.B. Dodiya, Y. Chu, T.G. Beach, C.H. Adler, et al., Disease duration and the integrity of the nigrostriatal system in Parkinson's disease, Brain 136 (Pt 8) (2013 Aug) 2419–2431 (PubMed PMID: 23884810. Pubmed Central PMCID: PMC3722357).

[3] J. Blesa, I. Trigo-Damas, M. Dileone, N.L. Del Rey, L.F. Hernandez, J.A. Obeso, Compensatory mechanisms in Parkinson's disease: Circuits adaptations and role in disease modification, Exp. Neurol. 298 (Pt B) (2017 Dec) 148–161 (PubMed PMID: 28987461. Epub 2017/10/11. eng).

[4] D.W. Dickson, Parkinson's disease and parkinsonism: neuropathology, Cold Spring Harbor Perspect. Med. 2 (8) (2012) a009258 (PubMed PMID: 22908195. Pubmed Central PMCID: PMC3405828. Epub 2012/08/22. eng.).

[5] M.D. Cykowski, E.A. Coon, S.Z. Powell, S.M. Jenkins, E.E. Benarroch, P.A. Low, et al., Expanding the spectrum of neuronal pathology in multiple system atrophy, Brain 138 (Pt 8) (2015 Aug) 2293–2309 (PubMed PMID: 25981961).

[6] P. Redgrave, M. Rodriguez, Y. Smith, M.C. Rodriguez-Oroz, S. Lehericy, H. Bergman, et al., Goal-directed and habitual control in the basal ganglia: implications for Parkinson's disease, Nat. Rev. Neurosci. 11 (11) (2010 Nov) 760–772 (PubMed PMID: 20944662. Pubmed Central PMCID: PMC3124757. Epub 2010/10/15. eng).

[7] T. Wu, M. Hallett, The cerebellum in Parkinson's disease, Brain 136 (Pt 3) (2013 Mar) 696–709 (PubMed PMID: 23404337. Epub 2013/02/14. eng.).

[8] A.P. Strafella, N.I. Bohnen, J.S. Perlmutter, D. Eidelberg, N. Pavese, T. Van Eimeren, et al., Molecular imaging to track Parkinson's disease and atypical parkinsonisms: New imaging frontiers, Mov. Disord. 32 (2) (2017 Feb) 181–192 (PubMed PMID: 28150432. Epub 2017/02/06. eng.).

[9] M. Tahmasian, L.M. Bettray, T. van Eimeren, A. Drzezga, L. Timmermann, C.R. Eickhoff, et al., A systematic review on the applications of resting-state fMRI in Parkinson's disease: Does dopamine replacement therapy play a role? Cortex 73 (2015 Dec) 80–105 (PubMed PMID: 26386442. Epub 2015/09/20. eng.).

[10] P.G. Spetsieris, D. Eidelberg, Scaled subprofile modeling of resting state imaging data in Parkinson's disease: methodological issues, NeuroImage 54 (4) (2011 Feb 14) 2899–2914 (PubMed PMID: 20969965. Pubmed Central PMCID: PMC3020239. Epub 2010/10/26. eng).

[11] V.D. Calhoun, J. Liu, T. Adali, A review of group ICA for fMRI data and ICA for joint inference of imaging, genetic, and ERP data, NeuroImage 45 (1 Suppl) (2009 Mar)

(S163-72. PubMed PMID: 19059344. Pubmed Central PMCID: PMC2651152. Epub 2008/12/09. eng).
[12] S.M. Smith, P.T. Fox, K.L. Miller, D.C. Glahn, P.M. Fox, C.E. Mackay, et al., Correspondence of the brain's functional architecture during activation and rest, Proc. Natl. Acad. Sci. U. S. A. 106 (31) (2009 Aug 04) 13040–13045 (PubMed PMID: 19620724. Pubmed Central PMCID: PMC2722273. Epub 2009/07/22. eng).
[13] A. Zalesky, A. Fornito, E.T. Bullmore, Network-based statistic: identifying differences in brain networks, NeuroImage 53 (4) (2010 Dec) 1197–1207 (PubMed PMID: 20600983. Epub 2010/07/06. eng.).
[14] D. Eidelberg, Metabolic brain networks in neurodegenerative disorders: a functional imaging approach, Trends Neurosci. 32 (10) (2009 Oct) 548–557 (PubMed PMID: 19765835. Pubmed Central PMCID: PMC2782537. Epub 2009/09/22. eng).
[15] A. Vo, W. Sako, K. Fujita, S. Peng, P.J. Mattis, F.M. Skidmore, et al., Parkinson's disease-related network topographies characterized with resting state functional MRI, Human Brain Map. 38 (2) (2017) 617–630 (PubMed PMID: 27207613. Pubmed Central PMCID: PMC5118197. Epub 2016/05/22. eng).
[16] M. Niethammer, D. Eidelberg, Metabolic brain networks in translational neurology: concepts and applications, Ann. Neurol. 72 (5) (2012 Nov) 635–647 (PubMed PMID: 22941893. Pubmed Central PMCID: PMC4564117. Epub 2012/09/04. eng).
[17] F. Agosta, P. Valsasina, M. Absinta, N. Riva, S. Sala, A. Prelle, et al., Sensorimotor functional connectivity changes in amyotrophic lateral sclerosis, Cereb. Cortex 21 (10) (2011 Oct) 2291–2298 (PubMed PMID: 21368084. Epub 2011/03/04. eng.).
[18] G. Douaud, N. Filippini, S. Knight, K. Talbot, M.R. Turner, Integration of structural and functional magnetic resonance imaging in amyotrophic lateral sclerosis, Brain 134 (Pt 12) (2011 Dec) 3470–3479 (PubMed PMID: 22075069. Epub 2011/11/15. eng.).
[19] A. Feigin, C. Tang, Y. Ma, P. Mattis, D. Zgaljardic, M. Guttman, et al., Thalamic metabolism and symptom onset in preclinical Huntington's disease, Brain 130 (Pt 11) (2007 Nov) 2858–2867 (PubMed PMID: 17893097. Pubmed Central PMCID: PMC4455546. Epub 2007/09/26. eng.).
[20] S. Gilman, G.K. Wenning, P.A. Low, D.J. Brooks, C.J. Mathias, J.Q. Trojanowski, et al., Second consensus statement on the diagnosis of multiple system atrophy, Neurology 71 (9) (2008 Aug 26) 670–676 (PubMed PMID: 18725592. Pubmed Central PMCID: Pmc2676993. Epub 2008/08/30. eng).
[21] W. Sako, T. Abe, Y. Izumi, H. Yamazaki, N. Matsui, M. Harada, et al., Spontaneous brain activity in the sensorimotor cortex in amyotrophic lateral sclerosis can be negatively regulated by corticospinal fiber integrity, Neurol. Sci. 38 (5) (2017 May) 755–760 (PubMed PMID: 28150100. Epub 2017/02/06. eng.).
[22] K. Dashtipour, J.J. Chen, C. Kani, K. Bahjri, M. Ghamsary, Clinical Outcomes in Patients with Parkinson's Disease Treated with a Monoamine Oxidase Type-B inhibitor: A Cross-Sectional, Cohort Study, Pharmacotherapy 35 (7) (2015 Jul) 681–686 (PubMed PMID: 26139574. Pubmed Central PMCID: PMC5034746. Epub 2015/07/04. eng).
[23] N. Tzourio-Mazoyer, B. Landeau, D. Papathanassiou, F. Crivello, O. Etard, N. Delcroix, et al., Automated anatomical labeling of activations in SPM using a macroscopic anatomical parcellation of the MNI MRI single-subject brain, NeuroImage 15 (1) (2002 Jan) 273–289 (PubMed PMID: 11771995. Epub 2002/01/05. eng.).
[24] M. Gottlich, T.F. Munte, M. Heldmann, M. Kasten, J. Hagenah, U.M. Kramer, Altered resting state brain networks in Parkinson's disease, PLoS One 8 (10) (2013) e77336 (PubMed PMID: 24204812. Pubmed Central PMCID: PMC3810472. Epub 2013/11/10. eng).
[25] C.Y. Luo, X.Y. Guo, W. Song, Q. Chen, B. Cao, J. Yang, et al., Functional connectome assessed using graph theory in drug-naive Parkinson's disease, J. Neurol. 262 (6) (2015 Jun) 1557–1567 (PubMed PMID: 25929663. Epub 2015/05/02. eng.).
[26] Y. Koshimori, S.S. Cho, M. Criaud, L. Christopher, M. Jacobs, C. Ghadery, et al., Disrupted Nodal and Hub Organization Account for Brain Network Abnormalities in Parkinson's Disease, Front. Aging Neurosci. 8 (2016) 259 (PubMed PMID: 27891090. Pubmed Central PMCID: PMC5102897. Epub 2016/11/29. eng).
[27] F. Skidmore, D. Korenkevych, Y. Liu, G. He, E. Bullmore, P.M. Pardalos, Connectivity brain networks based on wavelet correlation analysis in Parkinson fMRI data, Neurosci. Lett. 499 (1) (2011 Jul 15) 47–51 (PubMed PMID: 21624430. Epub 2011/06/01. eng.).
[28] M.C. Wen, H.S.E. Heng, J.L. Hsu, Z. Xu, G.M. Liew, W.L. Au, et al., Structural connectome alterations in prodromal and de novo Parkinson's disease patients, Parkinsonism Relat. Disord. 45 (2017 Dec) 21–27 (PubMed PMID: 28964628. Epub 2017/10/02. eng).
[29] X. Suo, D. Lei, N. Li, L. Cheng, F. Chen, M. Wang, et al., Functional Brain Connectome and Its Relation to Hoehn and Yahr Stage in Parkinson Disease, Radiology. 285 (3) (2017 Dec) 904–913 (PubMed PMID: 28873046. Epub 2017/09/06. eng).
[30] M. Rubinov, O. Sporns, Complex network measures of brain connectivity: uses and interpretations, NeuroImage 52 (3) (2010 Sep) 1059–1069 (PubMed PMID: 19819337. Epub 2009/10/13. eng).
[31] M. Glickstein, N. Gerrits, I. Kralj-Hans, B. Mercier, J. Stein, J. Voogd, Visual pontocerebellar projections in the macaque, J. Comp. Neurol. 349 (1) (1994 Nov 1) 51–72 (PubMed PMID: 7852626. Epub 1994/11/01. eng).
[32] C. Habas, N. Kamdar, D. Nguyen, K. Prater, C.F. Beckmann, V. Menon, et al., Distinct cerebellar contributions to intrinsic connectivity networks, J. Neurosci. 29 (26) (2009 Jul 1) 8586–8594 (PubMed PMID: 19571149. Pubmed Central PMCID: PMC2742620. Epub 2009/07/03. eng).
[33] C.F. Lu, B.W. Soong, H.M. Wu, S. Teng, P.S. Wang, Wu YT. Disrupted cerebellar connectivity reduces whole-brain network efficiency in multiple system atrophy, Mov. Disord. 28 (3) (2013 Mar) 362–369 (PubMed PMID: 23325625. Epub 2013/01/18. eng).